NAVAL
POSTGRADUATE
SCHOOL

MONTEREY, CALIFORNIA

THESIS

EROSION IN SOUTHERN MONTEREY BAY

by

Juan R. Conforto Sesto

March 2004

Thesis Advisor: Edward B. Thornton
Second Reader: James MacMahan

Approved for public release; distribution is unlimited

THIS PAGE INTENTIONALLY LEFT BLANK

REPORT DOCUMENTATION PAGE				*Form Approved OMB No. 0704-0188*
Public reporting burden for this collection of information is estimated to average 1 hour per response, including the time for reviewing instruction, searching existing data sources, gathering and maintaining the data needed, and completing and reviewing the collection of information. Send comments regarding this burden estimate or any other aspect of this collection of information, including suggestions for reducing this burden, to Washington headquarters Services, Directorate for Information Operations and Reports, 1215 Jefferson Davis Highway, Suite 1204, Arlington, VA 22202-4302, and to the Office of Management and Budget, Paperwork Reduction Project (0704-0188) Washington DC 20503.				
1. AGENCY USE ONLY *(Leave blank)*		**2. REPORT DATE** March 2004	**3. REPORT TYPE AND DATES COVERED** Master's Thesis	
4. TITLE AND SUBTITLE: Erosion in Southern Monterey Bay			**5. FUNDING NUMBERS**	
6. AUTHOR(S) Juan R. Conforto Sesto				
7. PERFORMING ORGANIZATION NAME(S) AND ADDRESS(ES) Naval Postgraduate School Monterey, CA 93943-5000			**8. PERFORMING ORGANIZATION REPORT NUMBER**	
9. SPONSORING /MONITORING AGENCY NAME(S) AND ADDRESS(ES) N/A			**10. SPONSORING/MONITORING AGENCY REPORT NUMBER**	
11. SUPPLEMENTARY NOTES The views expressed in this thesis are those of the author and do not reflect the official policy or position of the Department of Defense or the U.S. Government.				
12a. DISTRIBUTION / AVAILABILITY STATEMENT **Approved for public release; distribution is unlimited**			**12b. DISTRIBUTION CODE**	

13. ABSTRACT (maximum 200 words)

The coastal cliff top line recession has historically been used to calculate erosion along the Southern Monterey Bay. Digital photogrammetry is used in this work to produce Digital Terrain Models (DTM), representing the coastal cliff top line of 1984. This links the historical recession data sets with the LIDAR measurements of 1997 and 1998 and a 2003 cliff top line measured using Kinematic DGPS. Recession time series starting in the 1940's are produced for several locations. Least square linear fits of the recession data are computed for the periods 1940-84, 1940-98 and 1940-03. At Fort Ord and Sand City the resulting slopes show a persistent erosion trend of ~1meter/year, unchanged in the last 19 years. The mean sea level (MSL) evolution is studied using historical San Francisco MSL data because of its high correlation with Monterey MSL. Higher MSL during El Niño years, coincident with higher erosion rates show the correlation between erosion and MSL. In the long term, high-erosion El Niño years combine with normal years averaging to a near constant erosion trend. For Phillips Petroleum and Beach Lab a significant decrease in the erosion rate is observed after sand mining stopped in Sand City.

Digital Photogrammetry provides a high-quality representation of the shoreline topography, offering useful information to the warfighter in terms of detailed beach or landing zone characterizations.

14. SUBJECT TERMS Coastal Erosion, Photogrammetry, El Niño, Southern Monterey Bay			**15. NUMBER OF PAGES** 53
			16. PRICE CODE
17. SECURITY CLASSIFICATION OF REPORT Unclassified	**18. SECURITY CLASSIFICATION OF THIS PAGE** Unclassified	**19. SECURITY CLASSIFICATION OF ABSTRACT** Unclassified	**20. LIMITATION OF ABSTRACT** UL

THIS PAGE INTENTIONALLY LEFT BLANK

EROSION IN SOUTHERN MONTEREY BAY

Juan R. Conforto Sesto
Lieutenant Commander, Spanish Navy

Submitted in partial fulfillment of the
requirements for the degree of

**MASTER OF SCIENCE IN METEOROLOGY AND PHYSICAL
OCEANOGRAPHY**

from the

**NAVAL POSTGRADUATE SCHOOL
March 2004**

Author: Juan R. Conforto Sesto

Approved by: Edward B. Thornton
                  Thesis Advisor

                  James MacMahan
                  Second Reader

                  Mary L. Batteen
                  Chairman, Department of Oceanography

                  Carlyle H., Wash
                  Chairman, Department of Meteorology

THIS PAGE INTENTIONALLY LEFT BLANK

ABSTRACT

The coastal cliff top line recession has historically been used to calculate erosion along the Southern Monterey Bay. Digital photogrammetry is used in this work to produce Digital Terrain Models (DTM), representing the coastal cliff top line of 1984. This links the historical recession data sets with the LIDAR measurements of 1997 and 1998 and a 2003 cliff top line measured using Kinematic DGPS. Recession time series starting in the 1940's are produced for several locations. Least square linear fits of the recession data are computed for the periods 1940-84, 1940-98 and 1940-03. At Fort Ord and Sand City the resulting slopes show a persistent erosion trend of ~1meter/year, unchanged in the last 19 years. The mean sea level (MSL) evolution is studied using historical San Francisco MSL data because of its high correlation with Monterey MSL. Higher MSL occurred during El Niño years, coincident with higher erosion rates show the correlation between erosion and MSL. In the long term, high-erosion El Niño years combine with normal years averaging to a near constant erosion trend. For Phillips Petroleum and Beach Lab, a significant decrease in the erosion rate is observed after sand mining stopped in Sand City.

Digital Photogrammetry provides a high-quality representation of the shoreline topography, offering useful information to the warfighter in terms of detailed beach or landing zone characterizations.

THIS PAGE INTENTIONALLY LEFT BLANK

TABLE OF CONTENTS

LIST OF FIGURES

THIS PAGE INTENTIONALLY LEFT BLANK

LIST OF TABLES

THIS PAGE INTENTIONALLY LEFT BLANK

I.   INTRODUCTION

Erosion along the western coast of the United States has been widely studied, particularly after the effects of the 1982-1983 El Niño winter. The focus of this study is the erosion along the Southern Monterey Bay shoreline. Sklavidis and Lima-Blanco (1985) and McGee (1986) studied historical erosion at selected locations in Monterey Bay during the period 1940-1984 using stereo photogrammetry techniques. McGee developed an empirical erosion model as a non-linear function of significant wave heights greater than 4 m. Wave heights were determined from the U.S. Army Corps of Engineers Wave Information Studies spectral wave climatology refracted to the 10 m contour. The mean standard error between observed and modeled erosion rates was ± 0.17 m/yr.

To accurately measure the anticipated morphologic shoreline changes along the coastlines of Oregon and California due to an El Niño event, pre and post-El Niño airborne Light Detection and Ranging (LIDAR) topographic maps of the shoreline were obtained by Sallenger (2002). As a result, a number of papers on erosion and morphology changes at particular coastal locations along the Oregon and California coasts have been written (see for example Sallenger et al. (2002)). Volumetric erosion was quantified along the shoreline. The alongshore spatial variability of the shoreline was also studied.

Sallenger et al. (2002) developed relationships between sea-cliff erosion and beach changes within pocket beaches in Central California based on the LIDAR surveys during the 1997-1998 El Niño winter. They observed that maximum sea-cliff erosion occurred where the width and elevation of the beach were minima. They also observed that there was a correlation between the magnitude of the sea-cliff retreat and the number of hours extreme wave run-up exceeded certain thresholds representing the protective capacity of the beach. A better correlation was obtained using a threshold representing the width of the beach rather than using a threshold representing the elevation of the beach. They present a model to scale sea-cliff retreat. The model predicts that the cliff

erodes the cross-shore distance that extreme wave run-up exceeded the pre-El Niño cliff position.

Revell, et al. (2002), using the same LIDAR data set, studied the El-Niño winter erosion in the Netarts Littoral Cell in Oregon. They observed that the largest erosion occurred in the embayments of large cuspate features where the beach was the narrowest.

Egley (2002) studied the erosion along the Southern Monterey Bay shoreline by comparing digital terrain models obtained before and after the 1997-98 El Niño winter from LIDAR data. The high-resolution digital terrain models allowed a precise computation of the erosion volume for the area studied.

A problem with the earlier works of Sklavidis and Lima-Blanco (1985) and McGee (1987) using photogrammetry to measure erosion in Southern Monterey Bay is the absolute horizontal datum is lacking, so there is no way to tie together thate work with Egley's (2002). A primary objective of this thesis is to provide continuity for the erosion study of the Southern Monterey Bay area. A method to solve this discontinuity is by repeating the earlier stereo photogrammetry in 1984 using the same horizontal datum of the LIDAR measurements.

Digital Photogrammetry provides a high-quality representation of the shoreline topography, offering useful information to the warfighter in terms of detailed beach or landing zone characterizations.

The next chapters describe the technique used to obtain the location of the cliff top line utilizing aerial photographs along the Southern Monterey Bay shoreline.

II. DIGITAL PHOTOGRAMETRY

A. DIGITAL PHOTOGRAMMETRY

Digital photogrammetry uses digital images to solve the geometrical problems of classical photogrammetry. However, the digital format of the images increases appreciably the possibilities of automation of the photogrammetry process. In this study, the PC-based software IMAGINE OrthoBASE is used to process the images. The output products are in digital format, such as orthophotos, Digital Elevation Models (DEMs), digital maps, etc. This allows these products to be imported into Geographic Information System (GIS) software.

B. AERIAL PHOTOGRAPHY

Aerial photographs are acquired with a plane flying stable and horizontal with the camera axis directed vertically downward. Photographs are taken so that there is usually a 60% overlap between consecutive images. The overlap area of the photographs is used to solve the geometrical relations to obtain 3D coordinates of the image points.

The photographs used here were taken by IK Curtiss on 12 April 1984. A set of 12 photographs were scanned by Spencer B. Gross Inc. at a 14-micron pixel resolution (1814 dpi) and then compressed to a 15:1 ratio in MrSID format.

C. INTERNAL ORIENTATION (CAMERA CALIBRATION)

The camera was a Wild RC8 with a nominal focal length of 153 mm. Camera calibration was performed at the Optical Science Laboratory of the National Mapping Division of the U.S. Geological Survey (USGS). This calibration is necessary to test the compliance of the camera with the specifications required by the USGS and to determine the internal geometry and deformation of the camera. The Calibration Report states the accurate geometric position of the reference marks called fiducial marks that appear on the bottom plate of the camera. These fiducial marks appear also on the photograph taken with the camera, allowing the internal orientation of the photos. The operator manually locates the fiducial marks on the photograph (on the screen of the

computer) and introduces the calibration data of the fiducial marks. Basically, this Internal Orientation process computes the size, position and orientation of the photograph plane relative to the aiming axis of the camera.

D. EXTERNAL CALIBRATION: MEASURING GROUND CONTROL POINTS (GCP)

To geo-reference the aerial pictures, it is necessary to know the 3-dimensional coordinates of at least three Ground Control Points (GCP) in the overlapping region of a pair of photos. This requires accurate measurement of points in the field. GCP's must be identified on the aerial images in order to introduce their coordinates into the program.

The GCP's were measured using Differential Global Positioning System (GPS). This technique requires a base station to be set-up over a known position, which is continuously recording data from the GPS satellites. The 'Rover' station records positions at the GCP location. A minimum recording time of 30 minutes is required at each GCP to obtain centimeter-accuracy. Post-processing combines the data from the 'Rover' station and the 'Base' station.

The best kind of GCP corresponds to clearly defined lines and corners where different types of surfaces meet (i.e. different color surfaces on the images, such as grass/concrete or sand/grass). This color contrast (gray tone for our case) and well defined crossing lines allows choosing a point on the photograph with just a few centimeters of error. Another aspect to consider is the age of the photographs. The aerial photos used for this work correspond to 1984. Since that time changes have occurred that made it difficult to identify points on the photos that are easy to find in the field. Finally, a set of possibly valid locations were determined and marked on the photos and the GCP collection began. Once in the field some of the points were dismissed because the features observed on the photos no longer exist. Most of the GCP were found and accurately measured.

The set of measured GCP in the overlapping area of a pair of photos allows the program to solve the geometrical relationship between photo pairs and ultimately calculate the position of every point in the image. Although only three

points are required, more points increase the accuracy in resolving the problem, which can be achieved by identifying Tie Points. Tie Points are points that can be identified on both photos of an overlapping pair, but whose coordinates are unknown. The program uses these Tie Points to refine the geometry resolution in that region of the photo. The program has an automatic Tie Point generation routine. As a digital image is a set of regularly spaced digital values of the corresponding gray-level value, it is possible to create algorithms to recognize homologous points (points that satisfy some properties in regard to a similarity measure, usually a linear correlation coefficient) on both images of the stereo pair. The program, after running the routine, lists all the points found likely to be homologous on both photos. A manual checking process of the points is required to dismiss incorrect matching points before accepting them. Additional Tie Points can be added manually. Adding Tie Points increases the accuracy of the orthophotos and Digital Terrain Models.

E.   DIGITAL TERRAIN MODEL (DTM) GENERATION

The most important product of the photogrammetry process is the Digital Terrain Model (DTM), which allows 3D interpretation of the surface. After the internal and external calibration is done, the program geometrically relates homologous points in both photos and calculates the 3D coordinates of those points.

Different types of digital matching algorithms (bilinear, bicubic, sinc, etc) are available for the automatic homologous points finding routine, and employ not only an individual pixel, but also the neighbors, to decide in a matching criterion. If the absolute orientation of the photo pair is available, as it is for our case after the internal and external calibration process, the digital matching computes the 3D coordinates of the matching points. In this manner, the program produces points whose three coordinates are accurately solved. There are several possible types of DTMs. The 3D-shape file DTM was chosen because of its compatibility with ArcView. The DTM generation by the computer is a costly process, requiring several computer hours.

F.   REFINING THE DTM: STEREO ANALYST

The DTM models produced are not very accurate in areas where it is difficult to find homologous points. In areas of uniform texture surfaces, such as sandy beach areas, the matching algorithm cannot find homologous points between photo pairs because the whole surface looks similar. The DTM produced shows low density of points in these areas. The problem is even worse when the algorithm identifies as homologous points that actually are not, which produces erroneous values of elevation for these points. As a result, the DTM shows mountains over the beaches in places that are actually flat or gently sloped.

For the sea surface the problem is even increased. The surface is not uniform in aspect because there is high contrast between dark sea surface and white foam from breaking waves. But, as the two photos of each pair are not taken simultaneously but with some time interval, the white features moved during that interval. As a result, when the algorithm looks for homologous points, it tries to match white features that are at different locations. The resulting DTM shows mountains representing the actually flat sea surface.

As the beach area is the most important for our study, these erroneous DTM values must be removed, and the actual values must be added to the model. The removing task can be done easily using ArcView software. The DTM model, using a 3D-shape file format, appears as sets of points having 3D coordinates. The easiest way to identify points with a wrong value is to lay them over the ortho-rectified image of the area. This way the sea surface points can be easily identified and removed from the file. The points over the beach surface corresponding to sandy areas with no contrast can be also identified and removed. The result of removing so many points is that we end up having a DTM file with little or no information within the beach surface. Therefore, we need to add points to represent this area. These points are added using 3D Analyst software, which is included in the digital photogrammetry Imagine 8.5 software. The 3D Analyst allows using stereographic vision for pairs of photos. The

previously produced ortho-rectified images are used for 3D viewing of the area. The image pair is superposed on the monitor screen color-filtered with red and blue. The operator using red-blue glasses (one color for each eye) can see each photo with the corresponding eye, creating the effect of having stereo, three-dimensional vision. The operator can identify and measure the elevations of different points.

Starting from overlapping pairs of ortho-rectified photos, the coastal cliff and beach area can be seen three-dimensionally. New sets of points are measured and added to the DTM. Measuring three-dimensional points using this technique requires acclimating your vision to the stereo model, and it takes time (sometimes days) to start to appreciate the volumetric features of the terrain. Measuring points is a slow process, mainly because the elevation of each point must be carefully evaluated before recording the coordinates. Points are measured along the cliff top, the cliff base and midway between the cliff and the shoreline.

The points over the sea surface are not measured using the 3D Stereo Analyst. Since the elevation of those points is already approximately known (Mean Sea Level at zero elevation) they are manually added uniformly over the sea surface using ArcView.

THIS PAGE INTENTIONALLY LEFT BLANK

III. LIDAR

A. AIRBORNE LASER SURVEYING

Airborne Topographic LIDAR Mapper (ATM) directly measures topography elevation by aircraft. LIDAR allows detecting and ranging remote objects based on the time-resolved sensing of light emitted and reflected. Pulsed LIDAR emits at ultraviolet to near infrared wavelengths. NASA ATM system uses blue-green wavelengths. This method allows relatively low cost geomorphic surveys at decimeter vertical accuracy and at spatial densities greater than one elevation measurement per square meter.

B. NASA ATM

In principle, laser surveying can be carried out from a satellite, aircraft, or fixed platform. For this work, data were obtained using the NASA ATM aircraft-mounted system. The configuration used by NASA is an aircraft equipped with a LIDAR instrument, Inertial Navigation System, and GPS, which is operated in tandem with a differential GPS base station. The aircraft flies along the coast at a height of approximately 700 m surveying a ground swath directly below the aircraft. A geodetic grade GPS receiver on board the aircraft records position throughout the flight. The aircraft GPS positions are later combined with a signal concurrently acquired by a nearby GPS base station for differential GPS post-processing that allows for determining the aircraft flight trajectory within 5 cm rms. The LIDAR scanning mechanism consists of a nutating mirror that produces an elliptical scan pattern. The off-nadir angle is 15 degrees with the swath roughly one-half of the nominal 700 m aircraft altitude approximately 350 m wide.

C. PROCESSING NASA ATM SURVEY DATA

1. ATM Positioning

LIDAR distances recorded during the ATM flight require further post-processing. Given the laser range errors of several centimeters, the aircraft location throughout a survey flight must be known within about 5 centimeters in order to measure topography to a desired accuracy of about 15 centimeters. As

explained above, an accurate position of the aircraft (and therefore of the LIDAR equipment) is recorded for each range measurement (Brock et al., 2002).

The accurate determination of the position of a spot over the terrain requires combining the accurate spatial position of the LIDAR with the measured range and applying the geometric solutions for the scan. NASA ATM can measure topography within 15 cm error (Sallenger et al., 2003). In order to achieve such a high accuracy a precise calibration is required.

2.   ATM Calibration

An in-situ pre-flight calibration of the laser ranger and the instrument angular mounting bias must be performed. The laser ranger calibration addresses the variability of the pulse amplitude received by the instrument. Before and after each flight, the laser beam is horizontally directed to a target at a known distance and ranges are recorded using different laser strengths. This provides the relationship between laser signal amplitude and range variation, allowing the elimination of systematic ranging errors.

The angular mounting bias calibration addresses attitude of the ATM relative to the other positioning equipment. This is performed by flying and recording data over a well-known surface, such as a previously surveyed parking lot, and comparing the resulting topographic data in the post-processing.

D.   DIGITAL TERRAIN MODEL GENERATION

The objective of the NASA ATM is to produce Digital Elevation Models (DEM). The ranging data recorded are used to obtain ground spots. In this process, the accurate spatial trajectory of the LIDAR combined with the measured ranges and the geometric equations of the scanning are used to compute ground spot coordinates. The set of computed spots have horizontal geodetic positions and ellipsoidal heights. The datum used for the surveys was WGS-84.

As a result of this process, a set of ground points is measured. Despite the non-uniform distribution of points, the result is a high density of points with spot

spacing varying between 1m to 5 m. This set of points forms the initial DEM obtained from LIDAR.

THIS PAGE INTENTIONALLY LEFT BLANK

IV.   DIGITAL TERRAIN MODEL (DTM) ANALYSIS

A.   GIS SOFTWARE: ARCVIEW 3.2

GIS software ArcView 3.2 developed by Environmental Systems Research Institute ESRI was used in this work. This software allowed generating different types of Digital Terrain Models (DTM) as well as obtaining cross-beach profiles for analysis.

B.   SURFACE MODELS

Surface models represent a continuous surface by means of a finite number of points. Points on the surface are obtained by interpolation algorithms. Different models involve using different number of neighbor points with different algorithms to interpolate a point. For this work we used mainly three types of models: 3D-shape models, TIN models and GRID models.

C.   3D-SHAPE FILES

The original source of points, for the digital-photogrammetry-generated DTM, are 3D-shape files. This type of file is convenient to work with using ArcView. 3D-shape files are sets of irregularly distributed points obtained by the automatic DTM generation algorithm in the digital photogrammetry process. The advantage of this format is that the points correspond to homologous points in the photo pair, and therefore, represent the shape of the terrain and retain its accuracy. This irregular distribution of the points is caused by the singularity of the terrain features. An area of more intricate terrain requires more points to be represented than a uniform, gently sloped area. TIN models exploit this advantage.

Using 3D-shape files, points can be manually added, erased and even edited to recalculate the elevation with respect to a new vertical datum. Editing is the main advantage. The original vertical datum of the photogrammetry data is the ellipsoidal elevation for WGS-84, as well as for the LIDAR data. Both data sets were transformed to a new vertical datum, the geoid surface or Global Geopotential Surface, which is close to the local Mean Sea Level. The elevation

field of the 3D-shape files was edited and the corresponding Global Geopotential Surface elevation was computed and added.
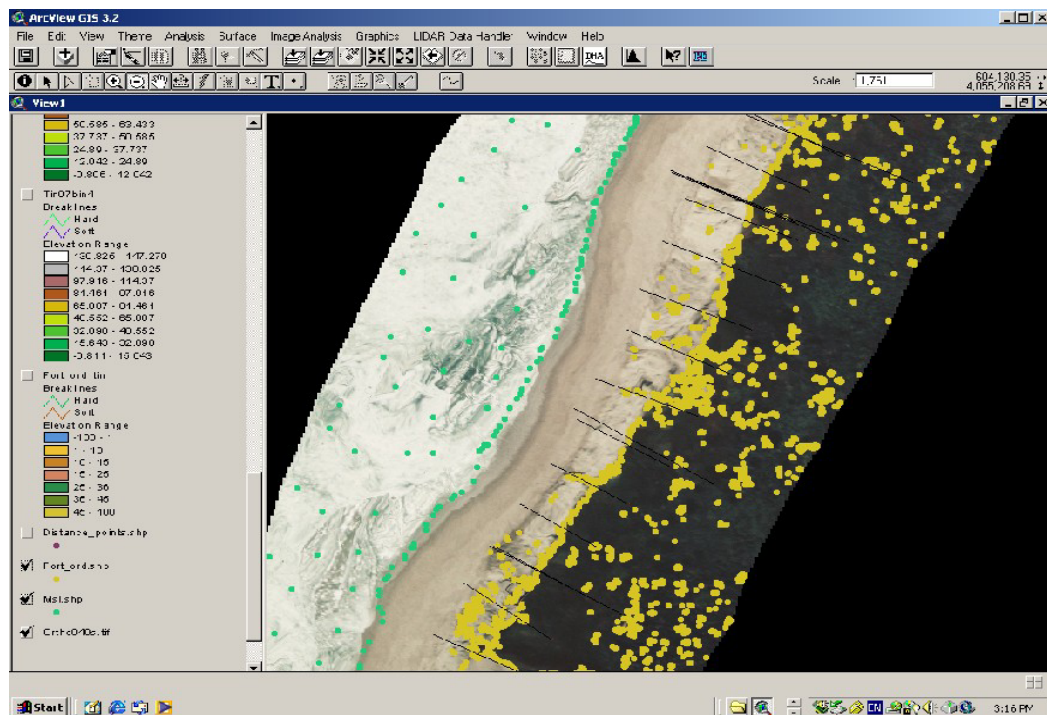

Figure 1.   3D-Shape model points over the South Fort Ord Orthophoto

Another editing process is erasing all the points generated over the sea on the DTM. This editing process is easily accomplished by laying the DTM points over the orthophotos. The points corresponding to the sea surface are identified and deleted. To replace these points, a new set of points is manually created. As our final vertical datum is close to the MSL, the elevation of the sea surface points is set to zero. This new set of points is used, in combination with the remaining DTM points, to create a new terrain model. Figure 1 shows the combination of the original model 3Dshape points and the manually added sea surface points.

D.   GENERATING A TIN MODEL

From the 3D shape files, a Triangular Irregular Network (TIN) model is generated, although the required model for analysis is a GRID model. This intermediate step of producing a TIN model is required to provide a continuous

3D surface to interpolate elevation data for the regularly spaced GRID model. Extracting a regularly distributed data GRID model directly from the 3D-shape model, would result in lost information, since the GRID model would have void areas with no information due to lack of points.
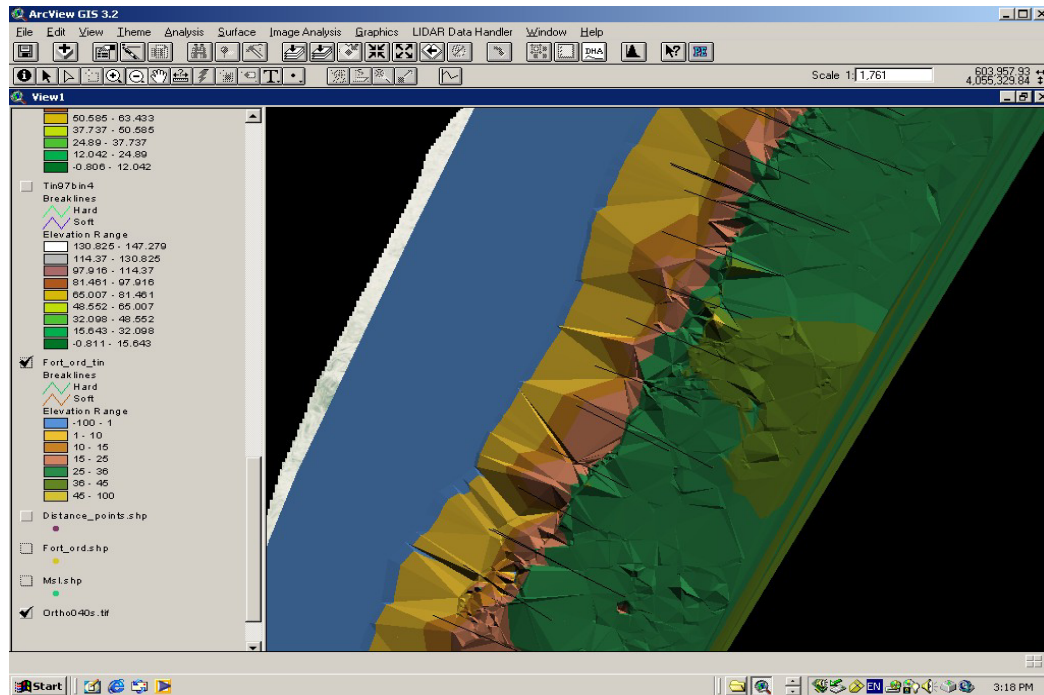

Figure 2.   TIN model of the South Fort Ord area

A TIN model is based on an irregularly distributed set of points. Any of the points contained in a TIN data set have three dimensions. These points are nodes. The surface is created by triangles whose edges are the lines between nodes. The irregular distribution of points allows increasing their density in areas of complex terrain and reducing their density in more regular terrain areas. The points, or nodes, correspond to singular points on the terrain and retain its position and elevation, allowing the original precision of the points to be conserved. Typically TIN models are used for high precision modeling of small areas, such as in engineering applications.

One of the more convenient aspects of TIN models is that it can be generated from a single set of points or can be generated by adding several sets

15

of points from different sources. For our case, the digital photogrammetry points obtained over the sea had wrong elevation, and we deleted them as explained before. Then we created a new set of points over the sea surface. We used both sets of points simultaneously to generate our TIN models.

E.   GENERATING A GRID MODEL

The ultimate model generated is the GRID model. A GRID model is a regular distribution of cells, a grid, with elevation values. Using ArcView, the elevation assigned to each cell is interpolated from the elevation of the TIN surface over it. Inverse Distance Weighting (IDW) is used to interpolate each grid point. The resolution of the GRID model produced depends on the size of the generated grid cells. For our case the grid size is 1 meter.

V.   PROFILING THE GRID MODELS

A.   EXTRACTION OF PROFILES USING ARCVIEW 3.2

As explained, GIS software ArcView 3.2 was used to extract profiles from the GRID models. This software allows selecting one or several GRID models simultaneously and extracting the elevation values corresponding to a line traced over the model by the user.

1.   Extracting Profiles

ArcView extracts a table of elevation (z) values from the GRID model corresponding to the grid cell x,y locations crossed by the traced line. If more than one grid model is selected, as is for our case, the figure presents the elevation profile curves of all the grids models allowing comparison between them. For our work we used grid models corresponding to 1984, 1997 and 1998.

2.   Obtaining the Recession Distance: Finding the Cliff Top

In previous erosion studies, it has been established that the best way to measure permanent erosion is to measure the distance the cliff top edge receded. During times of simultaneous high tides and storm waves the cliff toe is eroded. As a cliff is undercut, it eventually collapses. The sand fallen from the cliff is then washed away by the waves. The final shape of the cliff is similar to the previous one, but with recession of the cliff top due to the lost sand.

The easiest way to measure permanent erosion is to measure the distance between the locations of the cliff tops at two different years. Caution must be taken because this assumption will work only for coastal areas having a well defined cliff edge. For our area of interest there are some parts of the coast that comply with this condition, but there are some other areas that do not, such as areas of bare sand dunes. The loose sand forming the dunes does not produce sharp cliffs but rounded shapes. In addition, wind moves the sand dunes. The displacement of the dunes due to the wind will hide the effect of the erosion. Identifying permanent erosion on bare sand dune areas is more difficult.

As a consequence, in previous studies, the erosion has been measured in areas of sharp cliff top only, most easily identified on vegetated cliffs. Analytical photogrammetry was used in these studies to identify the cliff top. Using stereovision the edge of the cliff was identified and their coordinates obtained. In order to continue the erosion time series obtained in the past, we also focused our study on the same sharp cliff top areas. However, as our technique allows obtaining a profile of the terrain, it was possible to compare profiles from different years. In most cases, even for rounded sand dune areas, it was possible to visually identify similar shapes and to measure the corresponding recession distance. This is not as accurate as for a sharp cliff top, but it allows recession measurement for most of the coast shoreline.
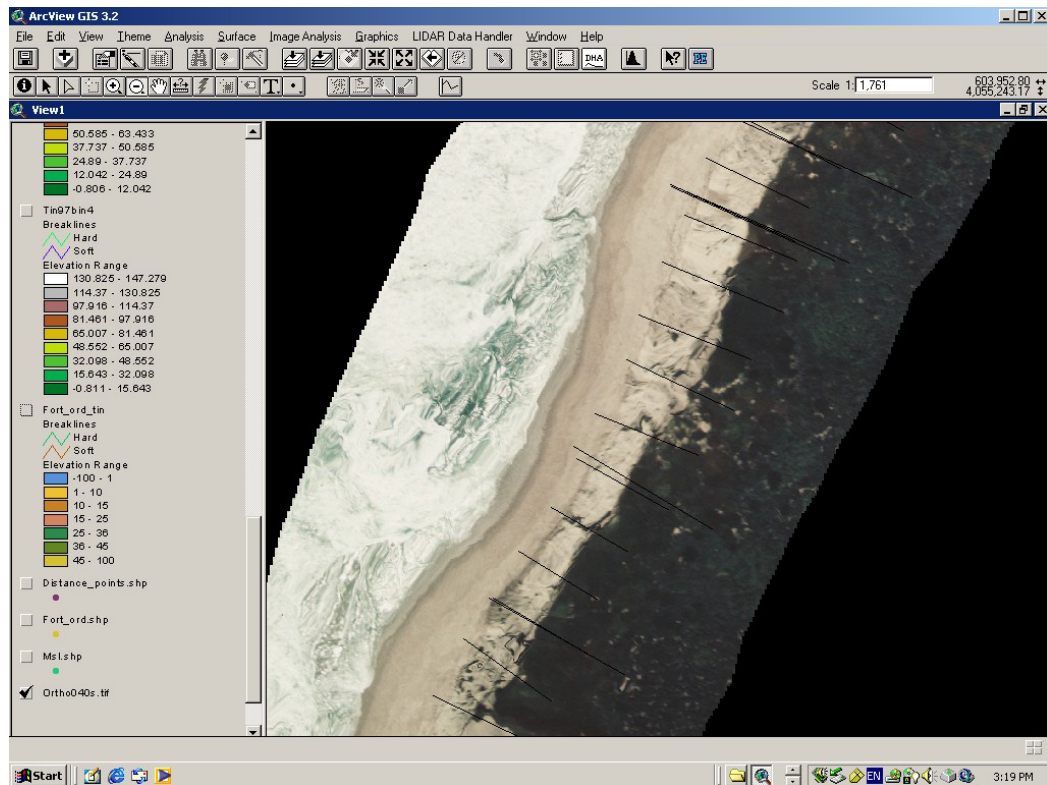

Figure 3.   South Fort Ord Orthophoto and profile lines

3.   Averaging the Cliff Top Recession

The cliff top recession is not a uniform process, as can be inferred from the previous explanation of the erosion process. It can not be determined from

18

the models whether a cliff is about to collapse or if it has just collapsed. The collapse will imply usually a few meters of recession. Measuring the cliff top recession at a single location (a single profile) may give an erroneous value of the recession rate. A collapsed cliff or an about to collapse cliff, provides quite different values. An average of many profiles for the same area is computed to reduce background noise.
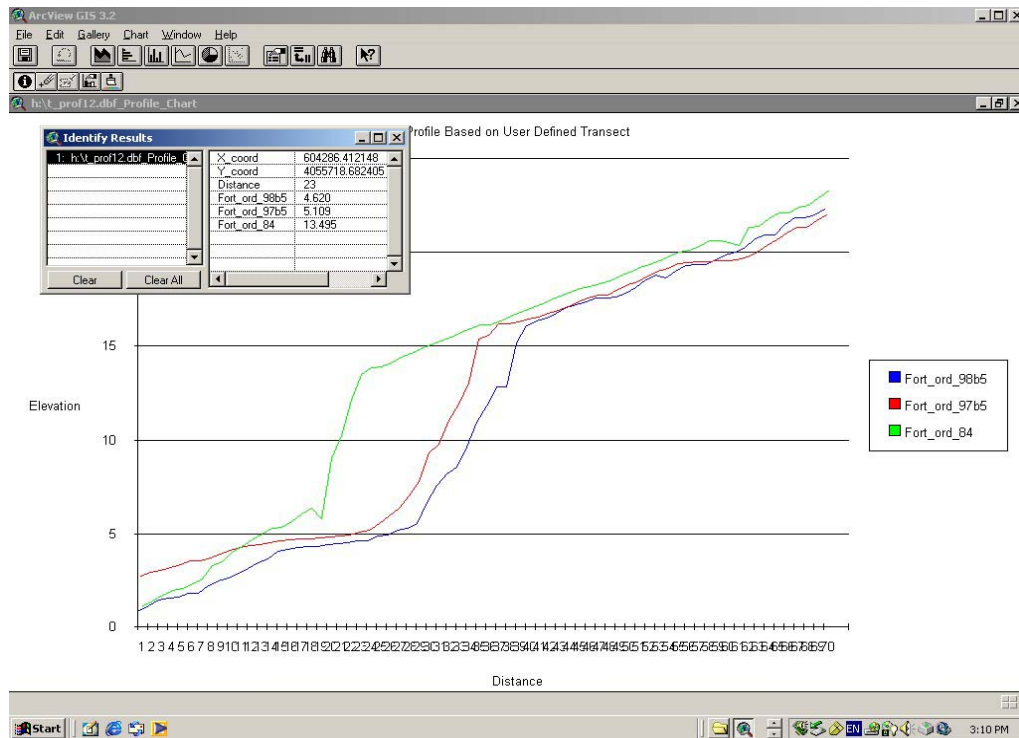

Figure 4.   South Fort Ord: profiles of the 1984, 1987 and 1988 GRID models. Horizontal axis shows values between 0 and 70 m. Vertical axis shows values between 0 and 25 m.

For our study of the South Fort Ord area, 59 profiles were extracted every 25 meters along the shoreline. The profiles were taken shore normal to the cliff line. This shore normal line was visually selected by observing the shape of the shoreline. For each profile, we obtained the x-y coordinates of the cliff top at 1984, as well as the elevation and the distances to the cliff tops at 1997 and

19

1998. The recession distances were averaged and an annual recession rate obtained.

B.   OBTAINING THE 2003 CLIFF-TOP LINE

The 2003 line was obtained by walking the cliff-top with the Kinematic DGPS 'rover' station mounted in a backpack. The recorded points were transformed from geographic to UTM coordinates using Geotrans2. The 2003 line is compared with the 1984 line, obtained from the profiles extracted from the DTM's with points spaced 25 meters along the coast. A corresponding point of the 2003 line was obtained. A minimum-distance criterion was used to determine the corresponding 2003-line point and the recession distance relative to the 1984 profile locations. The 1998-2003 recession distance was obtained by subtracting the 1984-1998 recession from the 1984-2003 distance.

VI.   DISCUSSION

A.   EROSION RESULTS

Erosion at four locations within Southern Monterey Bay, South Fort Ord, Sand City, Phillips Petroleum and Beach Lab, are examined (Figure 5). South Fort Ord is the most representative of the erosion process, because is open to the waves coming from the ocean and has historically shown intense recession. The other three locations were affected by the sand mining industry that took place at Sand City and Marina (Figure 5) up through the 1980's. The effect of sand mining plants closing is examined.
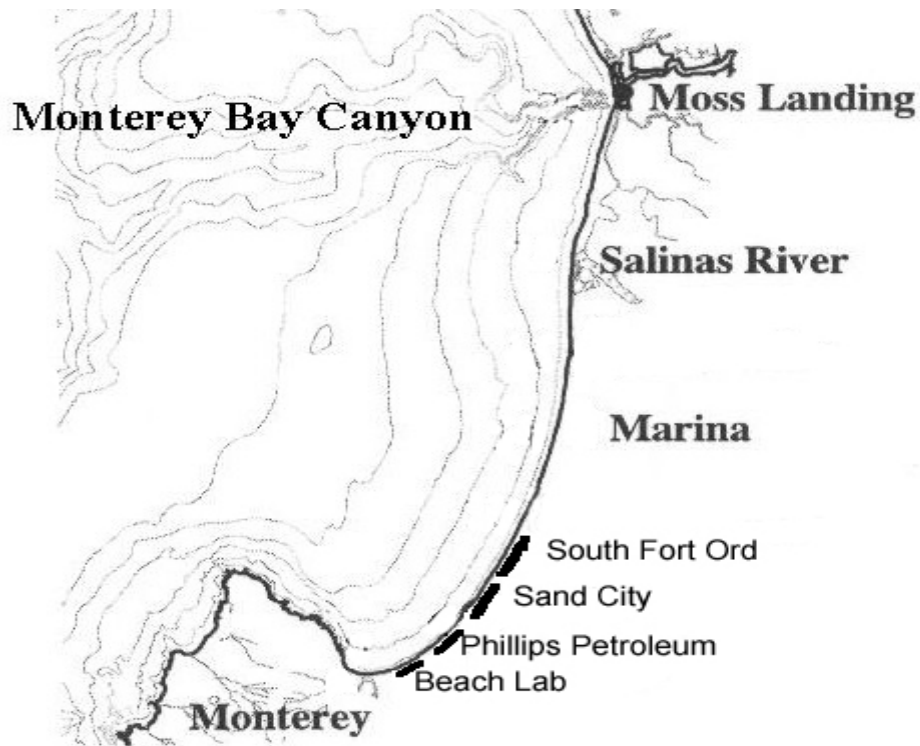

Figure 5.   Southern Monterey Bay

B.   PRODUCING GRAPHS OF THE RECESSION PROCESS

In previous studies, the recession distances for various years were obtained using analytical photogrammetry. To continue the recession distance time series, the old recession data are combined with values obtained for the period 1984-2003. A cumulative recession distance table is produced. The

accumulated recession distance starting in 1940 (or 1946, depending on the historical data set available) up to 2003 is presented. To better understand the evolution of the recession process, a least-squares linear fit is computed for the periods 1940-1984, 1940-1998 and 1940-2003. These best-fit lines show how the recession trend evolves over time.

C.   SOUTH FORT ORD

The historical recession at South Fort Ord from 1940 to 1984 is used (McGee, 1986). The historical time series is completed up to 2003. The linear slopes are 0.98 meters/year for 1940-1984, 0.99 meters/year for 1940-1998 and 1.01 meters/year for 1940-2003 (Figure 6). The three slopes are statistically similar, and it is concluded that the recession rate has not changed since 1984.
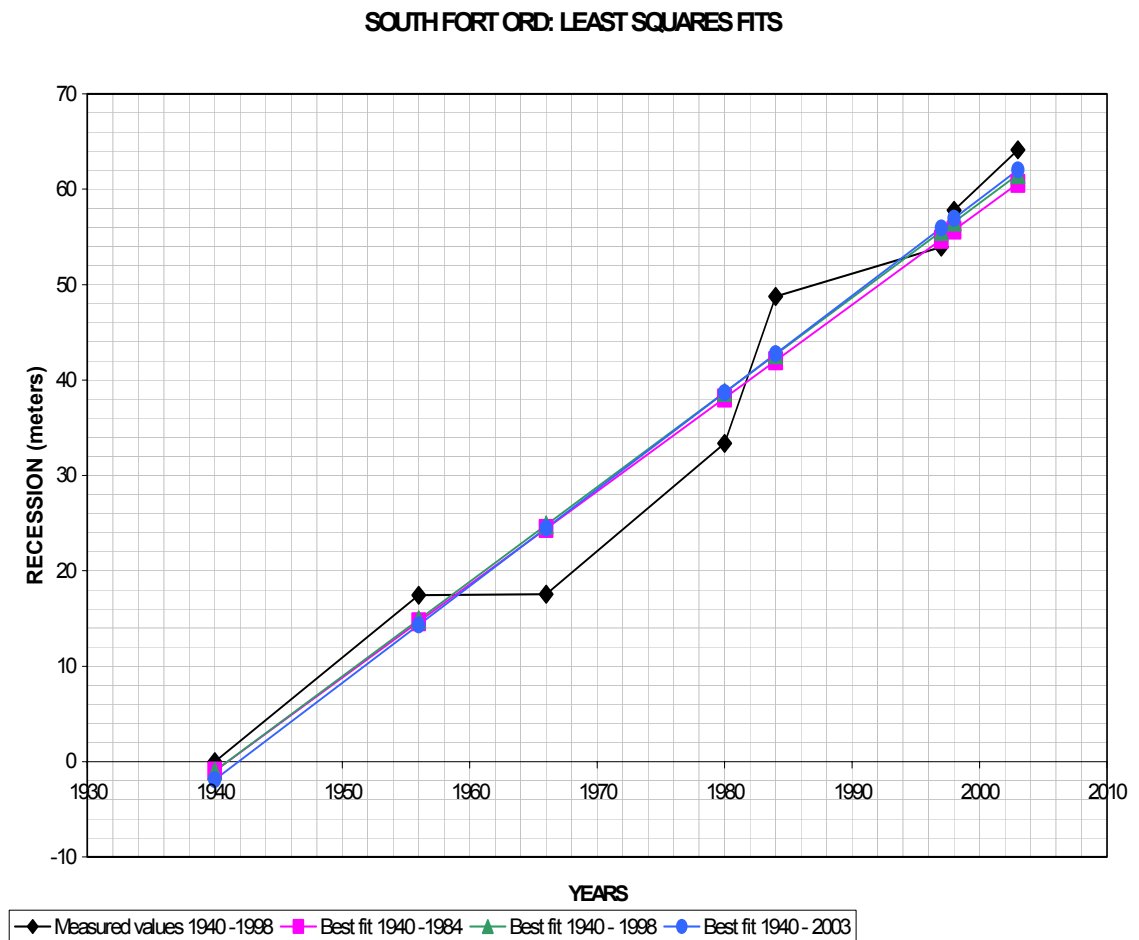

Figure 6.   South Fort Ord Recession and Least Squares Lineal Fits

22

Erosion Rate Results for South Fort Ord				
Data from	Time Interval	Recession Rate meters/year	Accumulated recession (meters)	Coast length in meters
McGee (1986)	1940 – 1956	1.09	17.44	692
	1956 – 1966	0.01	17.54	692
	1966 – 1980	1.13	33.36	692
	1980 – 1984	3.85	48.76	692
This research	1984 – 1997	0.40	53.94	1475
	1997 – 1998	3.85	57.79	1475
	1998 - 2003	1.27	64.13	1475
TOTAL	**1940 – 2003**	**1.02**	**64.13**	

Table 1.   South Fort Ord Recession Data

Since the recession rate did not change after adding the 19-year period (1984-2003) to the time series, it is concluded that combining different techniques of analytical photogrammetry, digital photogrammetry terrain modeling and LIDAR terrain modelings produces similar results. The unchanging recession rate also indicates that the erosion processes may not have changed since 1940. Erosion depends primarily on the sea level and the significant wave height. The available significant wave height data start in the 1980's, giving only a short record. On the other hand, the mean sea level time series is much longer, and therefore is examined to understand erosion processes.

1.   Sea Level at Monterey and San Francisco

The sea level record at Monterey started in 1973. However, the San Francisco sea level records started in 1853. The available records correspond to monthly-averaged mean sea level. To examine if the San Francisco sea level record can be substituted for Monterey, the two records are compared from 1973 to 2003 (Figure 7). From the regression analysis, a mean of –0.26 and slope of 0.77 are obtained with a correlation coefficient of 0.9. Therefore, the San Francisco record can be used to infer sea level at Monterey with a reduced elevation of approximately 0.8.
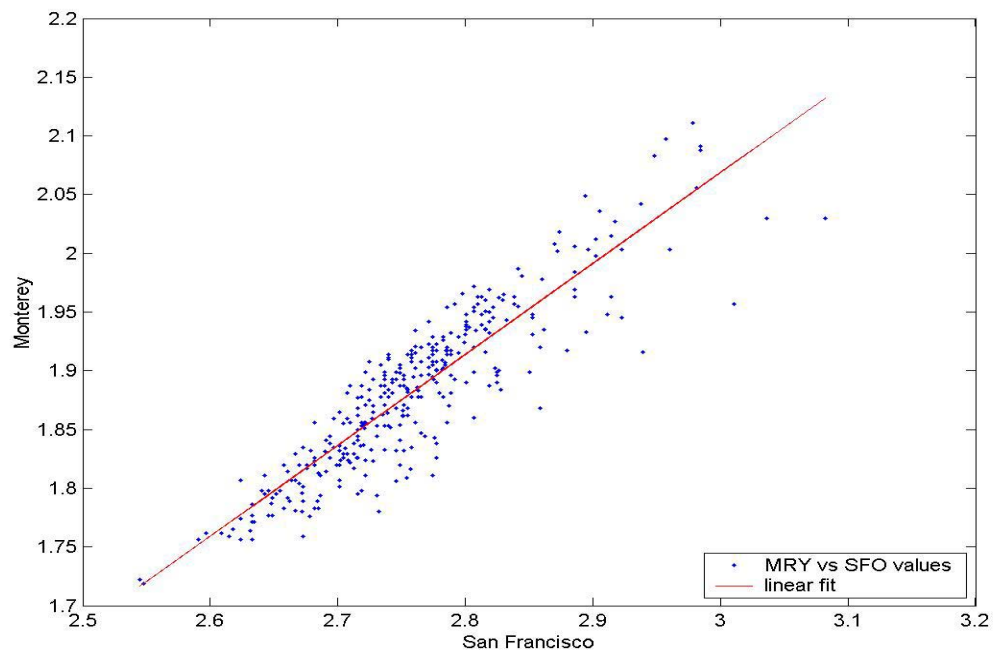
Figure 7.   Regression of Monterey MSL with San Francisco MSL giving a slope of 0.77, intercept of –0.26 and a correlation coefficient of 0.9.
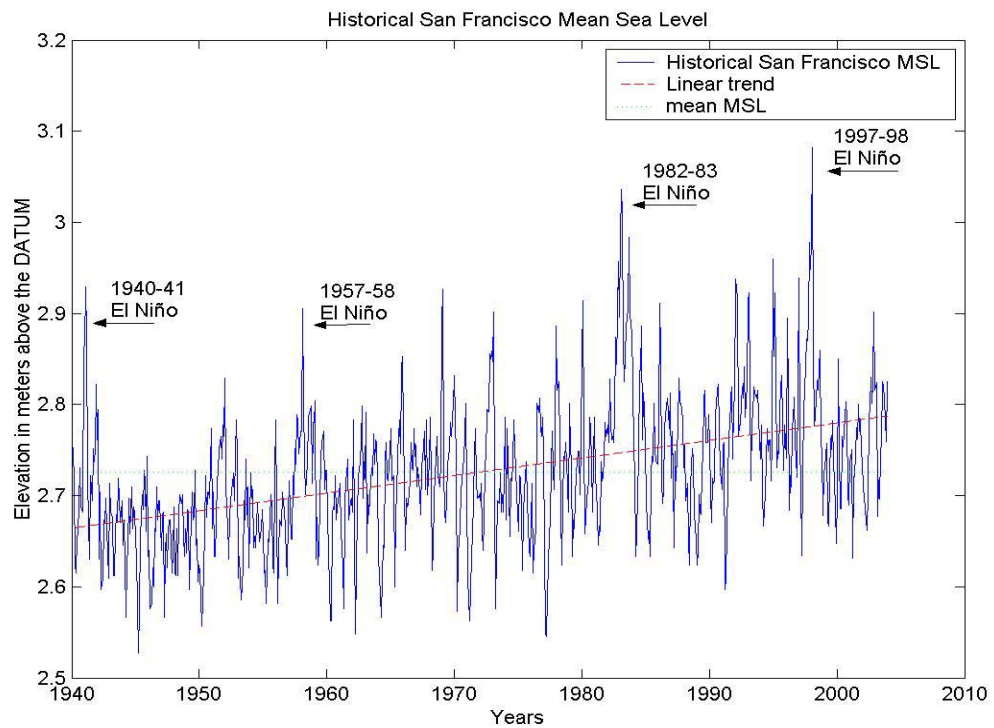

Figure 8.   Historical monthly averaged MSL at San Francisco relative to station Datum

2.   The Evolution of the MSL Trend

The San Francisco MSL record clearly shows variations coincident with El Niño events (Figure 8). These El Niño signals have been marked in the corresponding MSL spikes (Ryan et al.).

To answer the question whether MSL trends are increasing using the San Francisco record, least square linear fits were computed for the 1940-1984 period and compared with the 1940-2003 period. The resulting slopes are 2.31 mm/year for 1940-1984 and 1.93 mm/year for 1940-2003 (Figure 9), which are not statistically different at the 95% confidence level. As there have been several El Niño events since 1940, they can be viewed as normal occurrences.
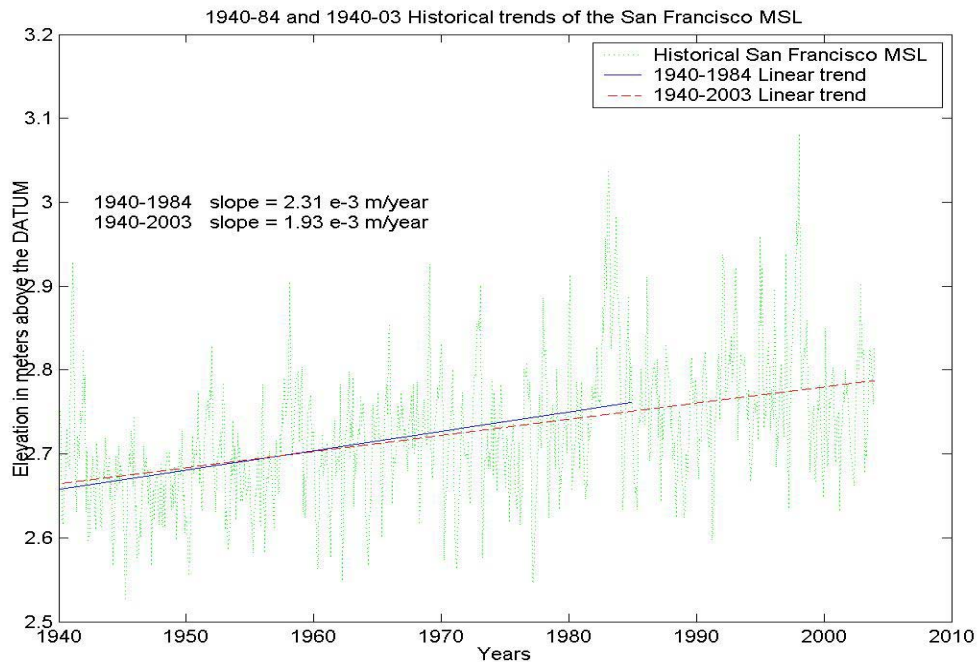

Figure 9.   Historical MSL trends relative to station Datum at San Francisco for 1940-84 and 1940-03

3.   Comparison of the Recession and the Mean Sea Level

The recession distance at South Fort Ord is compared with temporal changes in MSL. In Figure 10, the MSL has variations of millimeters (right ordinate), whereas recession distance is in meters (left ordinate).
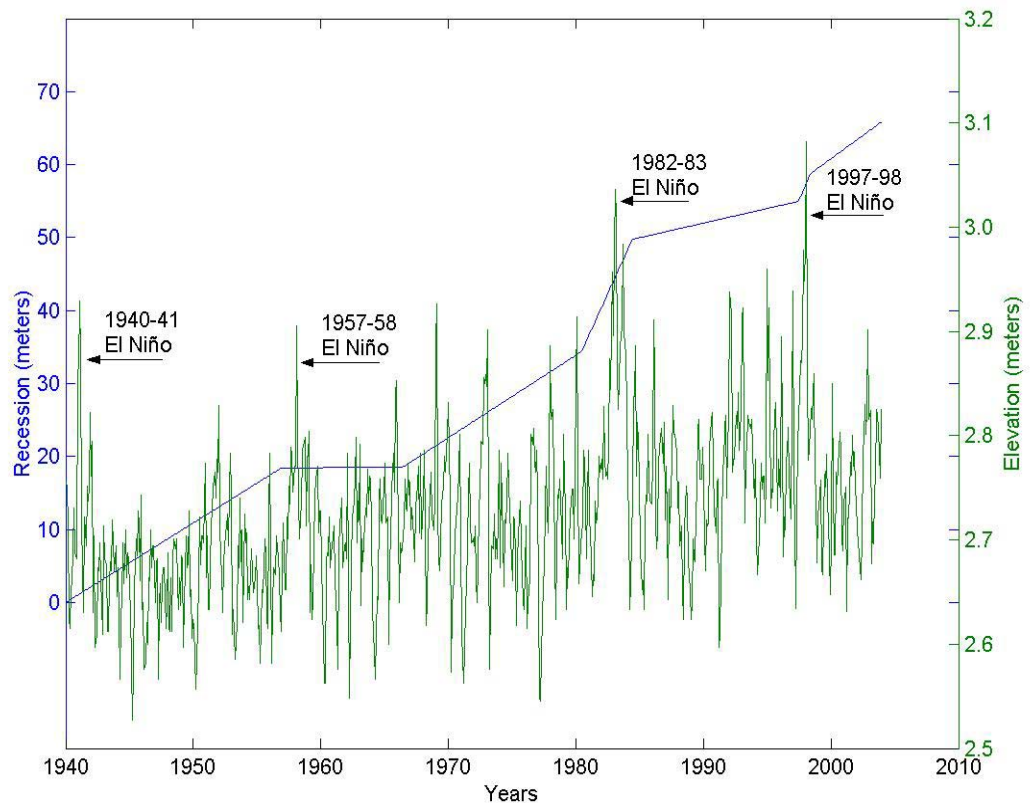
Figure 10.   South Fort Ord recession compared with San Francisco MSL

As can be seen in Figure 10, El Niño events are coincident with large erosion rates. This shows that coastal erosion is not a constant process but occurs episodically. Storms during El Niño events appear to be the main cause for coastal erosion. Large erosion occurs during El Niño winters, followed by several 'regular' years producing less erosion until a new El Niño event hits again, increasing recession. The long-term erosion rate composed of episodic El Niño high-erosion-rate years and 'regular' erosion years averages to a constant overall recession trend. The erosion rate and average MSL are compared in Figure 11. The average MSL has been rescaled to fit the comparison. Large erosion rates are coincident with El Niño events when the MSL is clearly higher.
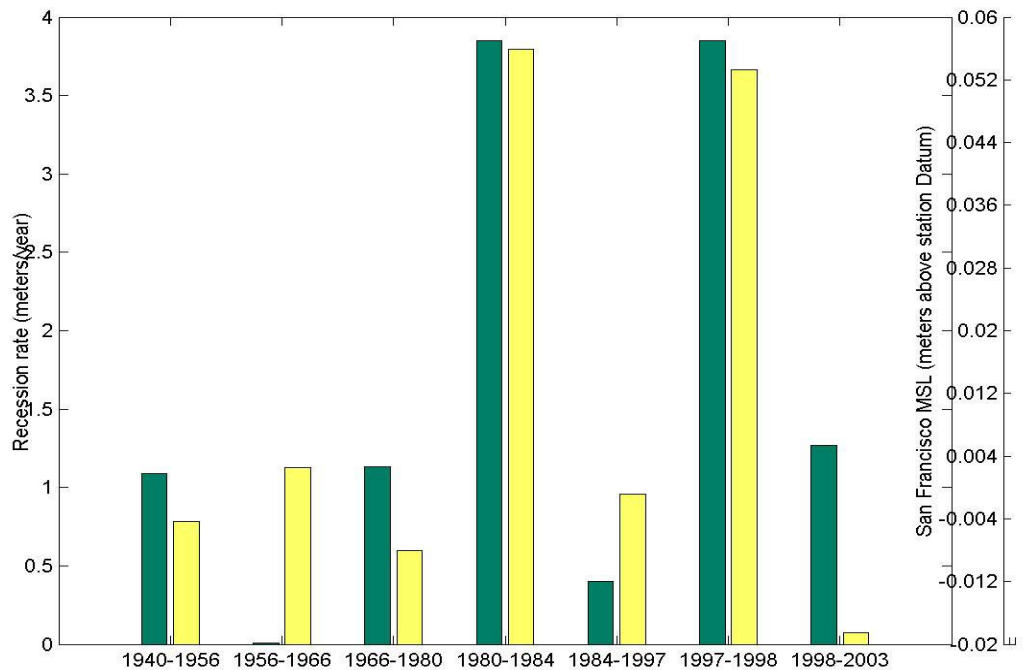
Figure 11.   Comparison of South Fort Ord Recession Rates and San Francisco average MSL for the same periods

D.   PHILLIPS PETROLEUM AND BEACH LAB

The historical recession data for the Phillips Petroleum and Beach Lab areas are available since 1946 (Sklavidis and Lima-Blanco, 1985). The recession time series were extended to 2003. As was done for Fort Ord, least-squares linear-fit lines are computed for the 1946-1984, 1946-1998 and 1940-2003 periods giving slopes of 0.61 m/year, 0.49 m/year and 0.47 m/year (Figure 12 and Table 2). For Phillips Petroleum the slopes are 0.75 m/year, 0.73 m/year and 0.72 m/year (Figure 13 and Table 3).

1.   Reduction in the Recession Rate

The evolution of the recession slopes indicates a reduction in the recession rate, which is more obvious for the Beach Lab case. After 1984 the recession rate appears to decrease and has been approximately maintained since then. At the Beach Lab the 1946-1984 slope is 0.61 m/year and the1984-2003 slope is 0.13 m/year, and at Phillips Petroleum the 1946-1984 slope is 0.75 m/year and the1984-2003 slope is 0.51 m/year. Although the 1984-2003 slope

values may be not very accurate because they correspond to a short period, they suggest a lower trend. It is hypothesized that the decrease in recession rate is associated with the cessation of sand mining along the Sand City shoreline in the 1980's.
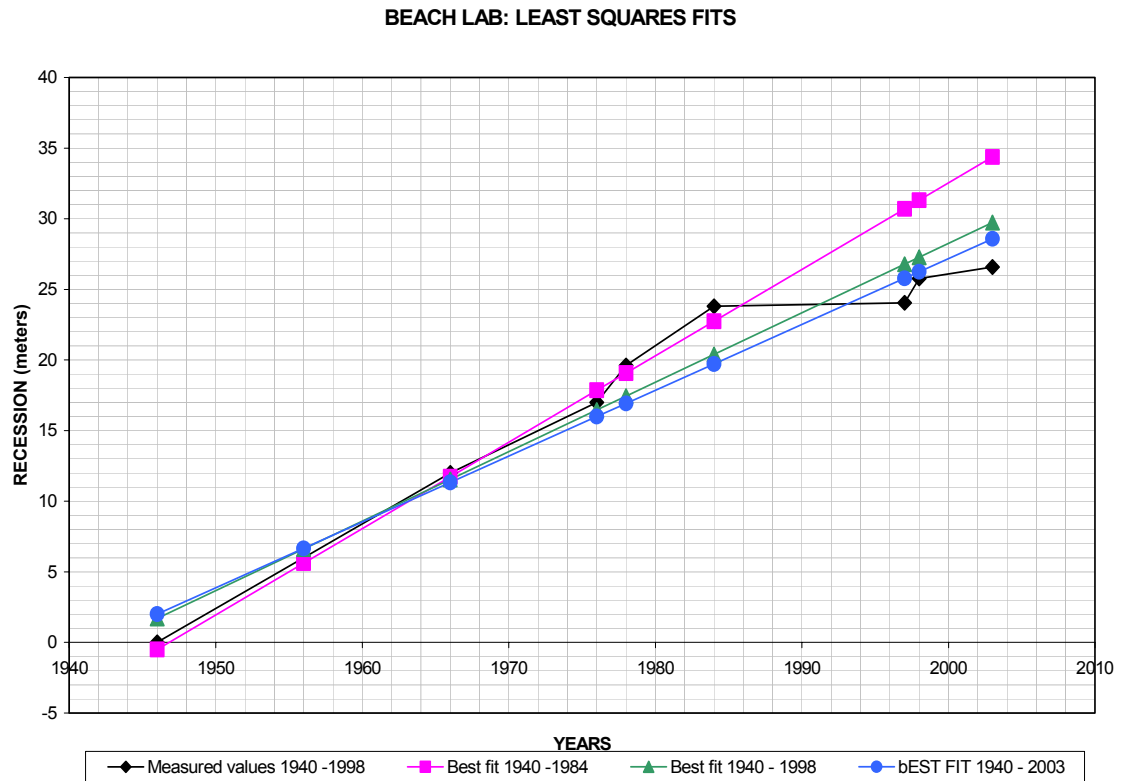
BEACH LAB: LEAST SQUARES FITS

Figure 12.   Beach Lab Recession and Least Squares Lineal Fits

Erosion Rate Results for Beach Lab				
Data from	Time Interval	Recession Rate meters/year	Accumulated recession (meters)	Coast length in meters
Sklavidis and Lima-Blanco (1985)	1946 – 1956	0.56	6	262
	1956 – 1966	0.59	12	262
	1966 – 1976	0.49	17	262
	1976 – 1978	1.30	19.6	262
	1978 – 1984	0.68	23.8	262
This research	1984 – 1997	0.02	24.05	1550
	1997 – 1998	1.72	25.77	1550
	1998 - 2003	0.16	26.57	1550
TOTAL	**1946 – 2003**	**0.47**	**26.57**	

Table 2.   Beach Lab Recession Data

2.   The Effect of Sand Mining

In the decade of the 80's, the sand mining industry ceased in the Sand City shoreline. Sand has been continuously extracted from the seabed within the breaker region, since about 1910. In this area, the sand is transported alongshore to the south due to the predominant waves from the Northwest. As Phillips Petroleum and Beach Lab are located south of Sand City, the sand mining intercepted sand being transported south. Griggs and Savoy (1985) suggests that sand mining reduced the availability of sand, which inhibits the formation of the offshore sand bars. Sand bars protect the beach by dissipating a majority of the winter storm wave energy within the surf zone. The lack of an offshore sand bar allows the wave energy to reach the shore and erode the beach face and dune cliff.
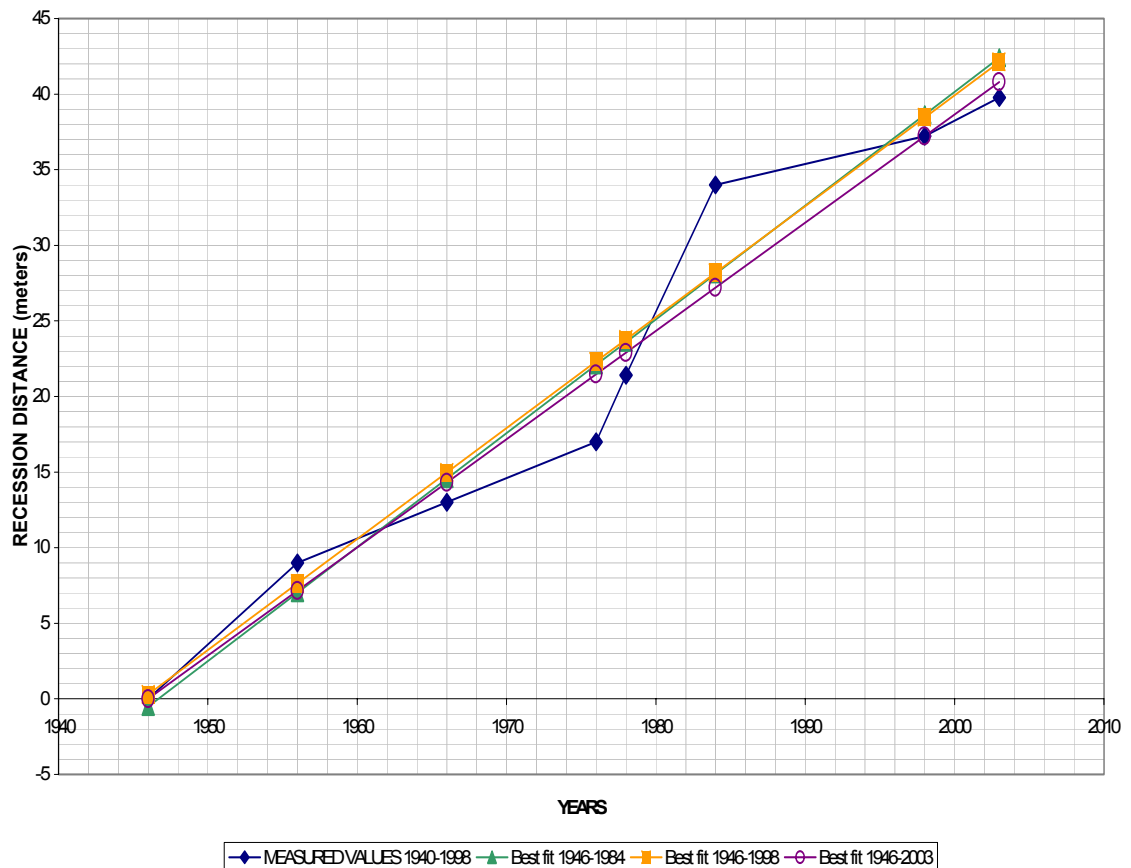

Figure 13.   Phillips Petroleum Recession and Least Squares Lineal Fits

Erosion Rate Results for Phillips Petroleum				
Data from	Time Interval	Recession Rate meters/year	Accumulated recession (meters)	Coast length in meters
Sklavidis and Lima-Blanco (1985)	1946 – 1956	0.9	9	204
	1956 – 1966	0.4	13	204
	1966 – 1976	0.4	17	204
	1976 – 1978	2.2	21.4	204
	1978 – 1984	2.1	34	204
This research	1984 – 1998	0.23	37.22	1350
	1998 - 2003	0.51	39.77	1350
TOTAL	**1946 – 2003**	**0.65**	**39.77**	

Table 3.   Phillips Petroleum Recession Data

E.   SAND CITY

The historical recession data for the Sand City area start in 1940 (McGee 1986). The recession time series was extended up to 2003. Least squares linear fit lines were computed for the 1940-1984, 1940-1998 and 1940-2003 periods giving slopes of 0.99 m/year, 1.01 m/year and 1.02 m/year (Figure 14 and Table 4).
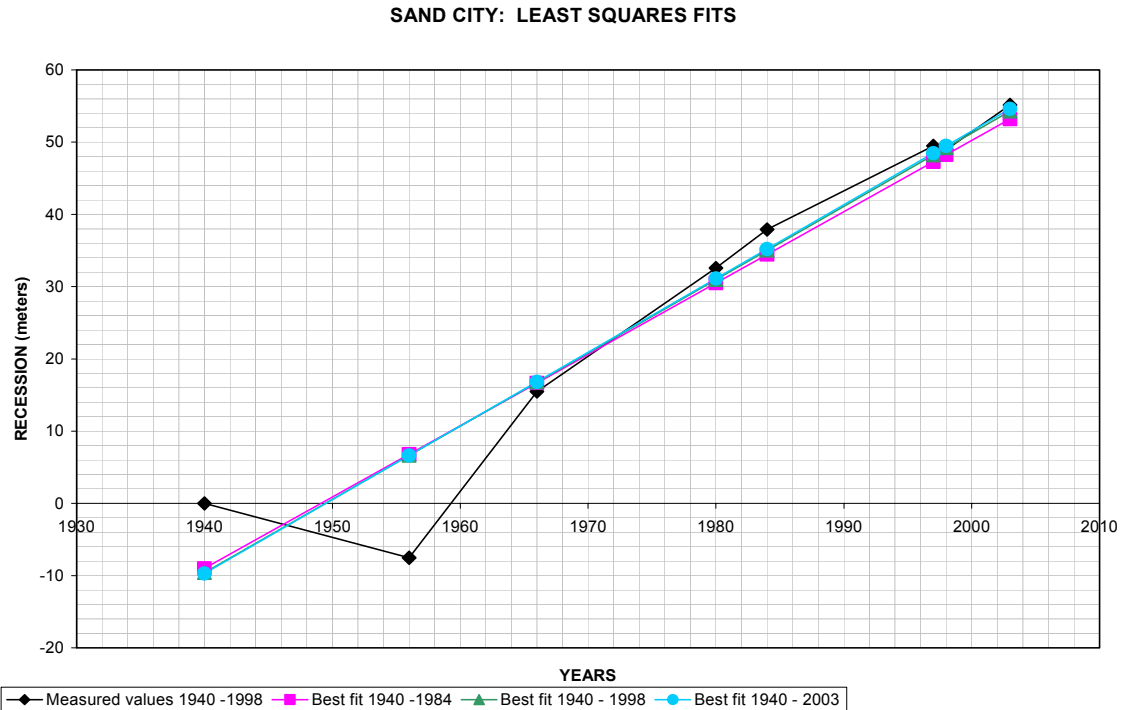

Figure 14.   Sand City Recession and Least Squares Lineal Fits

Erosion Rate Results for Sand City				
Data from	Time Interval	Recession Rate meters/year	Accumulated recession (meters)	Coast length in meters
McGee (1986)	1940 – 1956	-0.47	-7.52	540
	1956 – 1966	2.30	15.48	540
	1966 – 1980	1.22	32.56	540
	1980 – 1984	1.34	37.92	540
This research	1984 – 1997	0.89	49.49	550
	1997 – 1998	-0.55	48.94	550
	1998 - 2003	1.24	55.14	550
TOTAL	**1940 – 2003**	**1.06**	**55.14**	

Table 4.   Sand City Recession Data

As Sand City was an area of sand mining industry, man-made coastal shape changes occurred, which make it difficult to determine whether a natural cliff-top is present. For this reason, the specific locations of the sand mining operations have been skipped in the measurements, and only the natural cliff areas have been taken into account. Similar to South Fort Ord, the erosion trend slope shows small change when studying its evolution between 1984 and 2003. This may indicate that the erosion process here did not change appreciably during the period 1984-2003.

Although sand mining operations were centered in this area, no appreciable effects in the erosion trend can be observed after they ceased. This may indicate that the effects have been transferred to another location of the coast. As the alongshore sand transport is to the south in this area, the effects of sand mining would be observed in southern locations. This is consistent with the erosion trend changes observed for Phillips Petroleum and Beach Lab, which are located south of Sand City.

F.   SAND MINING

There have been several attempts to relate the volume of sand extracted by mining operations with volumes of sand eroded along the coast. Although they may be related, it is important to keep in mind that the main cause of erosion is the combination of high waves and tides. The estimated volume of sand mined per year in Sand City is compared with the recession rate (Figure 15). Changes in the recession rate are not reflected in the estimated volume of sand extracted.

In fact the larger erosion rates appear more related with El Niño events than with larger extraction volumes.

The erosion rate drop precedes the significant decrease in sand extraction (Figure 15). This may indicate that sand extraction influences erosion rates in a complex manner. The hypothesis that sand mining prevents the formation of the protective sand bar in winter may fit the observations. As a sand bar is in dynamic balance, the reduction in the supply of sand may break the balance preventing the formation of the bar. It is hypothesized that there is a threshold in the volume of sand extracted above which the sand bar is not formed and the beach is not protected of the winter waves. This could explain the drop in the recession rate seen in Figure 15 when there is still sand extraction in progress. Otherwise we would expect to observe a progressive decrease in the erosion rate simultaneous with the reduction in sand extraction.
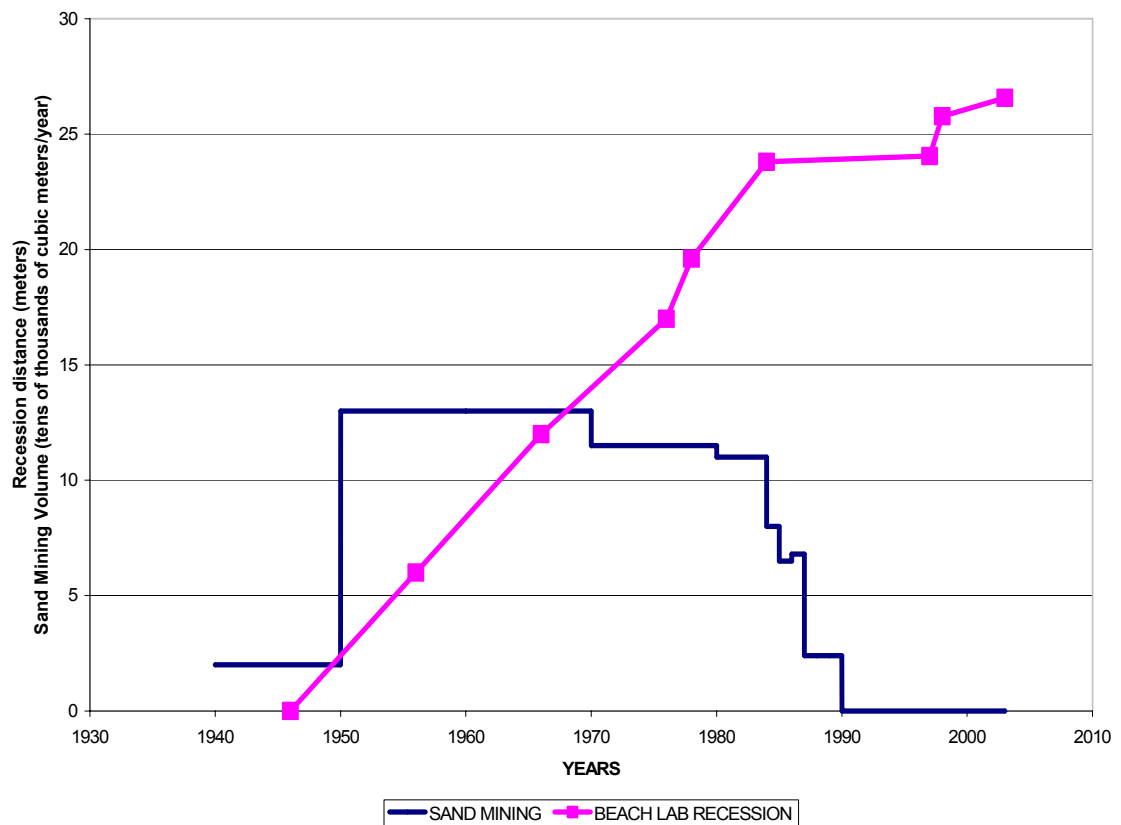

Figure 15.   Beach Lab Erosion rate vs. Sand City Mining.

Another aspect to consider about sand mining is the alongshore transport. As was seen, sand mining seems to influence locations to the south (Phillips Petroleum and Beach Lab) but not locations to the north (South Fort Ord or even the same Sand City). As sand mining can be seen as digging a hole within the surf zone, we can expect the hole to be filled with sand coming from both sides. As we do not observe any effect upstream in the erosion rate after ceasing sand mining, we can conclude that the alongshore transport of sand was large enough to feed the extraction process. Therefore we can estimate that the alongshore transport was larger than the volume of sand mined in Sand City.

An alternate explanation could be that the sand required to 'fill the hole' comes both from north and south. This implies that, when there was sand extracted, the direction of transport south of Sand City reverted, i.e. is to the north. This may also explain that the protective sand bar was not formed because the sand was transported alongshore to the north to 'fill the hole' caused by sand mining. In this case, when the volume of sand extracted is small enough to be supplied by the normal alongshore transport coming from the north, the sand in Beach Lab is again available to form the winter sand bar. That would explain the 'on/off' effect of sand mining in the erosion rate south of Sand City.

THIS PAGE INTENTIONALLY LEFT BLANK

VII. CONCLUSIONS

Based on combining the photogrammetry and LIDAR measures of cliff top erosion, it is concluded the two techniques give comparable results. The relative low cost of digital photogrammetry compared with LIDAR for digital terrain modeling suggest the value of using this technique for continuing erosion studies during times when no LIDAR mapping is available. Digital photogrammetry results show it is still a valuable tool for studying coastal erosion.

Digital Photogrammetry provides a high-quality representation of the shoreline topography, offering useful information to the warfighter in terms of detailed beach or landing zone characterizations.

Several recent papers indicate that the last two El Niño events (1983-84 and 1997-98) resulted in an increase in storm strength considering the historical time series. However, the constant overall erosion rate obtained for South Fort Ord and Sand City in this study indicates that there has been no acceleration in the long term erosion rates. Although during an El Niño winter increase the observed erosion rate, the previous and following years compensate for this increase with lower erosion rate, keeping the overall historical trend constant.

The historical mean sea level has been rising during the past 104 years. Although El Niño winters can be clearly identified in the historical MSL time series, there does not appear to be an increase in the rate of sea level rise.

The erosion rate appears to have decreased at Del Monte Beach in Monterey (Beach Lab) compared with the results obtained for South Fort Ord. It is hypothesized that the decreased erosion rate is associated with cessation of sand mining in Sand City in 1990. Sand mining intercepted the southerly transport of sand at Sand City, which reduced available sand to the beaches to the south. The sand extraction may have also reduced the supply of sand for the Del Monte Beach offshore bar, reducing, or eliminating its protective effect during winter storms (Griggs and Savoy, 1985). After sand mining stopped, the sand bar may have been regenerated. The increased transport of sand, besides

35

hypothetically regenerating the sand bar, provides sand and protects the beaches. The transport of sand could be responsible for the observed accumulating sand at Wharf #2.

LIST OF REFERENCES

Brock, J.C. et al. *Basis and Methods of NASA Airborne Topographic Mapper Lidar Surveys for Coastal Studies*. Journal of Coastal Research. 18 1 pp.1-13. Winter 2002.

Egley, L.A. *An Application of Lidar to Examine Erosion in the Southern Monterey Bay During the 1997-98 El Niño*. Master's Thesis. Naval Postgraduate School. Monterey. California. March 2002.

Griggs, G. and Savoy, L. *Living with the California Coast*, Duke University Press, 1985.

McGee, T. *Coastal Erosion Along Monterey Bay*. Master's Thesis. Naval Postgraduate School. Monterey. California. September 1986.

Revell, D.L. et al. *An Application of LIDAR to Analyses of El Niño Erosion in the Netarts Litoral Cell, Oregon*. Journal of Coastal Research. 18 4 pp.792-801. Fall 2002.

Ryan, H., Gibbons, H., Hendley II, J.W. & Stauffer, P. *El Niño Sea-Level Rise Wreaks Havoc in California's SF Bay Region.* [http://geopubs.wr.usgs.gov/fact-sheet/fs175-99/]. USGS Fact Sheet 175-99 Online Version 1.0. November 2003.

Sallenger, A.H. et al. *Evaluation of Airborne Topographic Lidar for Quantifying Beach Changes*. Journal of Coastal Research. 19 1 pp.125-133. Winter 2003.

Sallenger, A.H. et al. *Sea-Cliff Erosion as a Function of Beach Changes and Extreme Wave Runup During the 1997-1998 El Niño*. Marine Geology. 187 pp. 279-297. 2002.

Sklavidis, A.I., & Lima-Blanco, W.R. *Coastal Erosion Along Monterey Bay.* Master's Thesis. Naval Postgraduate School. Monterey. California. 2002.

THIS PAGE INTENTIONALLY LEFT BLANK

INITIAL DISTRIBUTION LIST

1. Defense Technical Information Center
    Ft. Belvoir, Virginia

2. Dudley Knox Library
    Naval Postgraduate School
    Monterey, California